Optical immersion as a tool for tissue scattering properties control

Alexey N Bashkatov, Elina A Genina, Valery V Tuchin

Department of Optics, Saratov State University, 155, Moskovskaya str, Saratov, 410026, Russia

E-mail: bash@optics.sgu.ru

1 Introduction

Recent technological advancements in the photonics industry have led to a resurgence of interest in optical imaging technologies and real progress toward the development of non-invasive clinical functional imaging systems [1-8]. Application of the optical methods for physiological-condition monitoring and cancer diagnostics is a growing field due to simplicity, low cost and low risk of these methods. The development of optical diagnostics, therapy and surgery techniques is very important for laser medicine. In clinical dermatology, oncology, gynecology optical methods are used widely for vessels imaging [9,10], detection, localization and treatment of subcutaneous malignant growths [3-6,7,11-17] and photodynamic therapy of various diseases [3,6,18-25]. In ophthalmology, for treatment of advanced glaucoma the transscleral cyclophotocoagulation is used [26,27]. For monitoring of cerebral activity, in cardiology and rheology the oxygenation and content of blood are very important parameters [9,10,28-38]. One important problem of application of optical methods in medicine deals with the transport of laser (light) beam through fibrous tissues such as skin dermis, eye sclera, dura mater, etc. Due to high scattering of visible and NIR radiation at propagation within these tissues, there are essential limitations on spatial resolution and light penetration depth for optical diagnostic and therapeutic methods to be successfully applied [3,4,6,7,14,17,29,39-50]. Control of the tissue optical properties is a very appropriate way to solve the problem. The temporary selective clearing of the upper tissue layers is the key technique for the structural and functional imaging, particularly for detecting local static or dynamic inhomogeneities hidden within a highly scattering medium.

The optical properties of a tissue effectively controlled at compression, dehydration, coagulation, or at application of other external and internal actions [3,6,18,28,40-46,51-86]. Such control means the change of the scattering or absorption properties of a tissue.

It is well known that the major source of scattering in tissues and cell structures is the refractive index mismatch between mitochondria and cytoplasm, extracellular media and tissue structural components such as collagen and elastin fibers [3,6,11,36,40,47,53-55,59,87-97]. The scattering properties of the fibrous tissues (such as skin dermis, sclera, dura mater, etc.) significantly changed due to action of osmotically active immersion liquids [3,6,28,40,42-45,53-56,59,60,62-86]. Administration of the immersion liquid having refractive index higher than that of tissue interstitial fluid induces a partial replacement of the interstitial fluids by the immersion substance and, thus, matching of refractive indices of tissue scatterers and the interstitial fluid. Osmotic activity of the immersion agent may cause tissue dehydration, what also equalizes refractive indices within the tissue. The matching of refractive indices, correspondingly, causes the decrease of scattering. As osmotic immersion liquids aqueous solutions of glucose [40,42,44,53-56,59,60,63,64,67,68,70,72-76,78,80-85], mannitol [28,40,55,68,78], propylene glycol [45,62,63,81], polyethylene glycol [42], glycerol [43,44,64,69,75,77,78,81-83,86], trazograph [42,64,65,66,81], verografin [62], etc. are used.

Aqueous glucose solutions are more widely used for the control of tissue scattering properties. Glucose solutions were used for optical clearing of the skin [44,64,69,72,73,75,78,84], sclera [42,63-67,70,74,78,80], dura mater [68,70,78,83], liver [40,54,55], blood [81,82], cell cultures and optical phantoms [40,56]. The possibility of application of mannitol solution for optical clearing of membranes

---

This Chapter dedicated to Prof R S Sirohi on his 60th birth anniversary

surrounding brain has been discussed by Chance et al. [28]. Influence of mannitol solution on liver has been shown in Refs. 40, 55. Increase of glucose or mannitol content in tissue reduces refractive index mismatch and, correspondingly, decreases the scattering coefficient. Measurement of the scattering coefficient allows one to monitor the change of glucose concentration in the tissue and blood that is very important for monitoring of diabetic patients [53,59]. Computer modeling shows that administration of glucose solution in tissue causes significant decreasing tissue scattering and increasing light penetration depth [60,85]. Influence of the glycerol on the skin optical properties has been demonstrated in Refs. 43,44,64,69,75,77,78,83.

Well known that action of hypo-osmotic liquids on the tissue causes tissue cells swelling, and application of hyper-osmotic solutions causes shrinkage process [40]. At the same time, swelling (i.e. increasing tissue hydration) by direct immersion in the bathing solutions was found to cause a significant loss of soluble protein and proteoglycans from the interstitial fluid of the fibrous tissue [98]. Thus, application of osmotically active liquids is accompanied by tissue swelling and shrinkage, which should be taken into account.

In spite of numerous investigations related to control of the tissue optical properties, the problem of estimating diffusion coefficient of immersion liquid in tissues has not been studied in detail. The knowledge of diffusion coefficients is very important for development of mathematical models describing interaction between tissues and osmotically active liquids, in particular, for evaluation of drug and metabolic agent delivery through tissue. Many biophysical techniques for study of penetration of various chemicals through living tissue and for estimation of the diffusion coefficients are available [99-112] but only a few techniques are applicable for estimation of the diffusion coefficient of the immersion liquids in living human tissue. The majority of the methods based on the fluorescence measurements or on the usage of radioactive labels for detecting matter flux. The optical method for estimating the diffusion coefficient of the immersion liquid in a tissue has been suggested by Tuchin et al. [42]. This method based on the measurements of temporal changes of the scattering properties of a tissue caused by dynamic refractive index matching. It can be used both for *in vitro* and *in vivo* measurements [42].

We present the results of *in vitro* and *in vivo* experiments on fibrous tissues optical properties control by administration of osmotically active immersion agents such as glycerol, aqueous glucose and mannitol solutions. As typical fibrous tissues the skin, sclera and dura mater have been studied. The experiments show that action of these osmotically active immersion liquids makes these tissues more transparent. Basing on temporal dependencies for tissue scattering coefficients obtained from time-dependent optical transmittance measurements the diffusion coefficients of glucose and mannitol in skin, sclera and dura mater have been estimated. The presented results summarize the investigations performed by authors of the paper and their colleagues (Dr. Yuri P Sinichkin, Dr. Vyacheslav I Kochubey, Nina A Lakodina et al. from Saratov State University, Russia, and Dr. Igor V Meglinski from Cranfield University, UK). The results are general and could be used to describe optical clearing of other tissues.

2 Physical properties and structure of typical fibrous tissues

Fibrous tissues such as sclera, dermis and dura mater show similar structure and consequently, similar optical properties. These tissues consist mainly of conjunctive collagen fibers packed in lamellar bundles [42,113-115] that immersed in an amorphous ground (interstitial) substance containing glycosaminoglycans, proteins, and protein-polysaccharide complexes [116-118]. These fibrils arranged in individual bundles in a parallel fashion; moreover, within each bundle, the groups of fibers separated from each other by large empty lacunae distributed randomly in space [113]. Collagen bungles show a wide range of widths (1 to 50 μm) and thicknesses (0.5 to 6 μm) [113]. These ribbon-like structures are multiple cross-linked; their length can be a few millimeters [51]. They cross each other in all directions but remain parallel to the tissue surface. Fig. 1 shows structure of typical fibrous tissue [113]. The glycosaminoglycans play a key role in regulating the assembly of collagen fibrils and tissue permeability to water and other molecules [116-118]. In spite of similarity of the fibrous tissues, some differences in

Fig. 1 The typical electron photographs of scleral tissue (x2900) [113]

their structure took place due to the functions provided by these tissues in an organism. This requires to overview briefly main features of the structure of these tissues.

The sclera is the turbid nontransparent medium that covers about 80% of the eyeball and serves as a protective membrane. Together with the cornea, it allows the eye to withstand both internal and external forces to maintain its shape. The thickness of the sclera is various. It is thicker at the posterior pole (0.9 to 1.8 mm); it is thinnest at the equator (0.3-0.9 mm) and at the limbus is in the range of 0.5 to 0.8 mm [51]. The sclera reaches a maximum thickness at 30 to 40 years [119]. The age-averaged thickness for the posterior pole, equator and the limbus are 0.76, 0.45, and 0.56 mm (119 eyes, from 1 to 80 years old).

Hydration of the human sclera can be estimated as 68%. About 75% of its dry weight is due to collagen, 10% is due to other proteins, and 1% to mucopolysaccharides [51].

The sclera contains three layers: the episclera, the stroma, and the lamina fusca [51]. At the *in vivo* investigations, it is necessary to take into account the presence of the conjunctiva and Tenon's capsule (~200 μm in thick), which both cover the scleral tissue from the external side. They impede the immersion liquid penetration into the sclera and, consequently, decrease the degree of eye tissue clearing. The thickness of the scleral collagen fibers also shows regional (limbal, equatorial, and posterior pole region) and aging differences [113,115]. In the equatorial region of the eye collagen fibrils exhibit a wide range of diameters, from 25 to 230 nm [113]. The fibers in the scleral stroma have a diameter ranging from 30 to 300 nm [51]. Similar results for diameters have been obtained by other authors [120,121]. The fibrils' diameters also depend on age [120,121]: they are the smallest in childhood [120]. The average diameter of the collagen fibrils increases gradually from about 65 nm in the innermost part to about 125 nm in the outermost part of the sclera [115]; the mean distance between fibril centers is about 285 nm [122].

The episclera has a similar structure with more randomly distributed and less compact bundles than in the stroma. The lamina fusca contains a larger amount of pigments, mainly melanin, which are generally located between the bundles. The sclera itself does not contain blood vessels but has a number of channels that allow arteries, veins and nerves to enter or leave the eye [51]. The human sclera is the main part of eye tissue and defines its optical properties.

The dermis is the main component of skin, which is a complex and multilayer organ. The thickness and properties of the skin vary according to anatomical location [123-125]. In addition, there are considerable age-dependent changes in the structure [126], properties [127] and composition of the skin [128]. Simplified model of skin structure contains four layers: epidermis (~100 μm thick) and dermis (1-2 mm) subdivided, following the distribution of blood vessels in skin, into upper blood net plexus (~100 μm thick), reticular dermis (~1150 μm thick) and deep blood net plexus (~100 μm thick) [123,129-131].

The epidermal layer includes a stratum corneum and a living epidermis. The stratum corneum comprises approximately 15 cell layers. It is not homogeneous and the layers represent various stages of corneocyte and intercellular lipid maturation [123,124,132-135]. The stratum corneum is the permeability barrier to percutaneous absorption. Directly under the stratum corneum is the living epidermis, composed primarily of 10-20 layers of keratinizing epithelial cells, which are responsible for the synthesis of the stratum corneum [123]. The low layers of the stratum corneum have more water associated (30% by

weight), though both are considerably less well hydrated than the dermis (70% by weight) [136,137]. The living epidermis contains most of the skin pigmentation, mainly melanin, which is produced in the melanocytes. Random spatial distribution of melanin particles in the living epidermis affects both the scattering and absorption properties of human skin [138,139].

The dermis forms the bulk of the skin. The vast network of fibrous, filamentous and amorphous connective tissue determines the tensile strength and elasticity of the skin, and provides the physical support for extensive nerve and vascular networks. The dermis is primarily made up of collagenous fibers [140], that account for 70% of the dry weight of skin. The dermis has an extensive vascular blood and lymph network, which participates in various processes including nutrition, heat exchange, repair, immune responses and thermal regulation [141-144]. The optical properties of the dermis, mainly, absorption depend on the distribution of blood containing hemoglobin. Scattering properties of dermal layers are defined mainly by the fibrous structure of the tissue, where collagen fibers are packed in collagen bundles and have lamellae structure [138]. The mean diameter of collagen fibrils, which is approximately equal to 60 nm, is comparable with the mean distance between fibril centers.

Underlying the dermal layer is the subcutaneous fat, which is made up of a network of adipocytes (~120 μm in diameter) containing stored lipid oil in the form of single droplets of triglyceride and arranged in lobules. The collagen fibers permeate the hypodermis and interact with the dermis; it is very difficult to remove all of the subcutaneous fat from *in vitro* dermis samples [123].

Thus, the epidermis is compact, thin, predominantly light-absorbing layer, well-endowed with specific pigments for UV photoprotection by absorption. The dermis, in contrast, is a thick, relatively acellular layer in which light scattering plays a much more important role, with its absorption over much of the optical range, including UVA, localized largely in blood vessels [138].

Human dura mater is a protective membrane, which surrounds brain. It has a fibrous structure. Typically, with the age the dura mater thickness changes from 0.3 to 0.8 mm. As an object for light propagation, this is a turbid, non-transparent medium. It consists mainly of conjunctive collagen fibrils packed in lamellar bundles that immersed in an amorphous ground (interstitial) fluid [145,146].

Dura mater contains five layers: the external integumentary layer, the external elastin network, the collagen layer, the internal elastin network and the internal endothelium integumentary layer [145]. The collagen layer is the main layer of human dura mater. Thus, its optical properties defined mainly by the optical properties of the collagen layer. It is worth noting that those abrupt boundaries between upper, middle and lower layers are absent. Thus, according to its structure, human dura mater is the closest to the sclera and skin dermis. The main difference between the structure of sclera and dura mater is the presence of the branched net of blood vessels in dura mater [145].

The average diameter of the dura mater collagen fibrils has been estimated by us using the data presented by Spacek in *Atlas of Ultrastructural Neurocytology* [147]. Processing these data, we have found that the average diameter of the dura mater collagen fibrils is about 100 nm.

According to its composition, the dura mater interstitial fluid is very close to the interstitial fluid of skin dermis [148] and constitutes a clear, colorless liquid containing proteins, proteoglycans, glycoproteins, and hyaluronic acid. It is worth noting that these molecules are excellent space filters. Due to their glycosaminoglycan chains, these molecules concentrate negative charges. They are highly hydrophilic, and their presence can provide a selective barrier to the diffusion of inorganic ions and charged molecules [118,148].

To design the optical model of fibrous tissue, in addition to form, size and density of the scatterers (collagen fibrils) and the tissue thickness, we are able to have information on the refractive indices of the tissue components. In the visible spectral range, the wavelength dependence of the refractive index of the collagen fibrils of the human sclera $n_c(\lambda)$ approximated from the empirical data is the following [78]:

$$n_c(\lambda) = 1.439 + \frac{15880.4}{\lambda^2} - \frac{1.48 \times 10^9}{\lambda^4} + \frac{4.39 \times 10^{13}}{\lambda^6}, \quad (1)$$

where λ is the wavelength, nm. The corresponding wavelength dependence of the refractive index of the skin interstitial fluid $n_I(\lambda)$ has a view [78]:

$$n_I(\lambda) = 1.351 + \frac{2134.2}{\lambda^2} + \frac{5.79 \times 10^8}{\lambda^4} - \frac{8.15 \times 10^{13}}{\lambda^6}. \quad (2)$$

Taking into account the similar nature of the sclera, skin dermis and dura mater, we may assume that the refractive indices of the collagen fibrils and interstitial fluid for the studied fibrous tissues have the similar wavelength dependencies.

3 Materials and Methods

3.1 Experimental setups

All optical measurements were performed using a commercially available multichannel optic spectrometer LESA-6med (BioSpec, Russia). Scheme of the experimental setup is shown in Fig. 2. As a light source a 250 W xenon arc lamp with filtering of the radiation in the spectral range from 400 to 800 nm was used. During *in vitro* light transmittance measurements, the glass cuvette with the tissue sample was placed between two optical fibers with a core diameter of 400 μm and a numerical aperture of 0.2. One fiber transmitted the excitation radiation to the sample, and another fiber collected the transmitted radiation. The 0.5-mm diaphragm placed 100 mm apart from the tip of the receiving fiber was used to provide collimated transmittance measurements. Neutral filter was used to attenuate the incident radiation. The measurements have been performed every 30 sec during 15-20 min for different sclera and dura mater tissue samples. The experiments with the skin samples have been performed every 1 min at the beginning and every 5 min afterwards during about 120 min. Experimental error does not exceed 5% in the spectral range from 500 to 800 nm and 10% in the spectral range from 400 to 500 nm. All *in vitro* experiments have been performed with the human sclera and dura mater, and rat skin tissues samples at room temperature (about 20^0C).

Study of swelling of the tissue samples was performed by means of the time-dependent weight measurements. The torsion scales with the precision of 1 mg were used. The tissue samples have been placed in a cuvette with the aqueous glucose or mannitol solution and its weight has been measured every 2 min during 40 min.

In vivo reflectance measurements were performed using a fiber optical probe with a system of optical fibers. The fibers were enclosed in cone-shaped aluminum holder to provide a fixed distance between the fibers and tissue surface. Light from a stabilized light source (xenon arc lamp) was delivered to the tissue by means of the fiber fixed normally to the surface of tissue. The receiving fiber was displaced at angle of 20 degrees to the sending fiber in such a way as the irradiated area had a 5-mm diameter and the area of light collection had a 10-mm diameter.

The tissue reflectance spectra was measured against $BaSO_4$ plate as a reference. To register the reflectance spectra the fiber optical probe was placed on the surface of the tissue. The measurements were carried out in different time intervals. Three series of measurements were carried out on animals, and one series of measurements has been performed on a male-volunteer. For all studies the reflectance spectra have been registered every 1-2 min. Time for registration of a single spectrum was 200 msec. Total time for the measurements of the reflectance from rabbit eye sclera was 30 min (as a clearing agent the 40% aqueous glucose solution was used). Total time for measurements of the reflectance from human skin is 140 min (clearing agent was 40% aqueous glucose solution). In case of measurements of reflectance spectra from the rat skin the total time of measurements was 20 min (clearing agent was glycerol) and 105 min (as a clearing agent the 40% aqueous glucose solution was used).

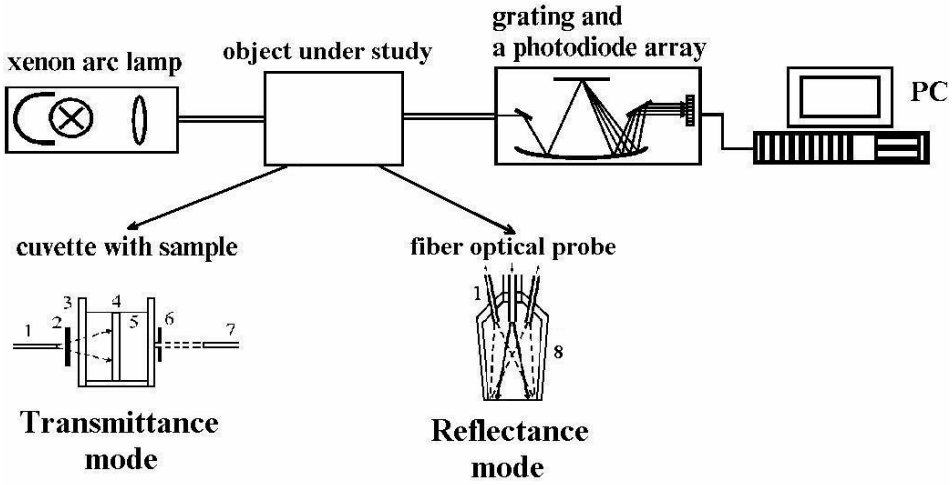

Fig 2 Experimental setup for measurements of collimated transmittance and reflectance spectra from tissue: 1 – optical irradiating fiber; 2 – neutral filters; 3 – cuvette; 4 – tissue sample; 5 – osmotically active immersion agent; 6 - the 0.5 *mm* – diaphragm; 7 – optical receiving fiber; 8 – aluminum holder.

3.2 The osmotically active immersion liquids preparation

As osmotically active immersion liquids the glycerol, aqueous glucose and mannitol solutions with different concentrations have been used. The concentrations of aqueous glucose solutions were 0.4 g/ml (40%), 0.3 g/ml (30%), and 0.2 g/ml (20%). Concentration of mannitol solution was 0.16 g/ml. Aqueous glucose solutions have been prepared using powder-like glucose monohydrate (ChemMed, Russia), and aqueous mannitol solution has been prepared using powder-like D-mannitol (Serva, New York, USA). Commercially available glycerol (ChemMed, Russia) was used in our experiments. The densities of the glucose solutions were measured as 1.07, 1.10, and 1.12 g/ml for concentration of glucose 20%, 30%, and 40%, respectively. The density of the mannitol solution was measured as 1.06 g/ml. The refractive indices of the clearing agents were measured by Abbe refractometer at wavelength 589 nm as 1.363 (0.2 g/ml), 1.377 (0.3 g/ml), 1.390 (0.4 g/ml) for glucose solutions, as 1.357 for mannitol solution, and as 1.450 for glycerol. pH of the solutions were measured by pH-meter "HANNA" (Portugal) as 6.05 for the mannitol solution, as 5.99 (0.2 g/ml), 5.91 (0.3 g/ml), 3.5 (0.4 g/ml) for the glucose solutions with different concentrations, and as 6.5 for the glycerol.

3.3 The tissue sample preparation for in vitro measurements

In this study, for *in vitro* measurements we have used samples of human sclera and dura mater, and rat skin. All human tissues were obtained by autopsy within 24 hours *post mortem*. After enucleation, the sclera samples were placed in saline. Before experiments the conjunctiva and the ciliary body as well as the retina with choroid were removed removed. The dura mater samples were kept under temperature -12^0C and before experiments have been unfrozen. The rat skin samples were obtained by autopsy within an hour *post mortem*. Hairs were removed from skin surface using tweezers. Before experiments all tissue samples have been cut into pieces with the area about 10×10 mm^2. The thickness of each tissue sample was measured at initial moment with a micrometer in ten points and averaged. The tissue samples have been fixed on a plastic plate with a square aperture 5×5 mm^2 and have been placed in a 5-ml cuvette filled up with the immersion agent.

3.4 In vivo measurements of tissue clearing

The *in vivo* studies of tissue clearing were performed with the rabbit eye sclera, rat skin and skin of a male volunteer. The animals have been anaesthetized by an injection of 1%-*natrium ethaminal* solution (40 mg/kg of animal weigh) prior to procedure. The measurements started in 30 min after the injection.

The rabbit's age was 5 months and its weight was 1.5 kg. Aqueous glucose solution with concentration 0.4 g/ml was used as a clearing agent. The solution was dropped onto the eye ball surface. The total volume of the used solution was 3 ml. The measurement of dynamics of the optical clearing started in 3 min after the solution administration onto the eye surface.

The preliminary *in vivo* investigations of skin clearing were done with white rats. The age of the rats was about 9 months and their weight was about 200 g. Removing hairs was done before the experiments. The 40%-glucose solution or glycerol (0.1 ml) was injected into the skin dermis in the area of a thigh. The measurement of dynamics of the optical clearing started in 1 min after the injection. Final studies of skin clearing were performed with skin of a male-volunteer. The intradermal injection of aqueous 40%-glucose solution by volume of 0.1 ml was done in the area of a forearm.

4 Experimental results

In this section, we present experimental results of *in vitro* and *in vivo* tissue clearing. During the process, the collimated transmittance (*in vitro*) and the backreflectance (*in vivo*) spectra of the tissues (such as skin, sclera and dura mater) have been measured concurrently with administration of different immersion agents (such as glycerol, aqueous glucose and mannitol solutions).

To understand the mechanisms of the scleral tissue optical clearing we have investigated *in vitro* the collimated transmittance spectra and change of the scleral sample weight concurrently with administration of glucose solutions. Figure 3 illustrates dynamics of the transmittance spectra. It is seen easily seen that the untreated sclera is poorly transparent for the visible light. Glucose administration with concentration 0.4 g/ml makes this tissue highly transparent, for example, up to 18% at 750 nm for the sample kept in solution for t = 5 min. The corresponding plots for time-dependent collimated transmittance at different wavelengths are presented in Fig. 4.

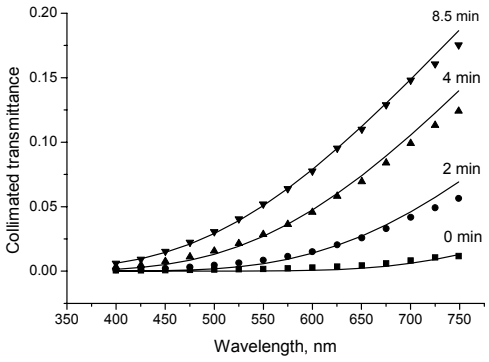

Fig. 3 The temporal collimated transmittance spectra of the human sclera sample measured *in vitro* concurrently with administration of 40%-glucose solution [63].

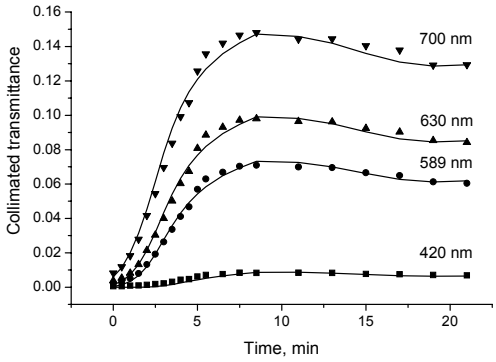

Fig. 4 The time-dependent spectral components of collimated transmittance of the human sclera sample measured *in vitro* concurrently with administration of 40%-glucose solution [63].

They show the dynamics of tissue clearing. It as well seen that the characteristic time response of human sclera optical clearing is about 5 min. In the figures symbols correspond to experimental data [63],

and a solid line corresponds to data calculated using the presented model (see below, Section 5). When applied as a clearing agent of aqueous glucose solutions with concentrations 0.2 g/ml and 0.3 g/ml [67] similar results were obtained but the degree of tissue clearing is less in comparison with 40% glucose solution. The collimated transmittance increased in about 4 fold at wavelength 700 nm for 20% glucose solution and collimated transmittance increased in about 5 fold for 30% glucose solution. For all glucose solutions, approximated time of maximal scleral clearing is about 8 min. It is worth noting that for *in vitro* application of these glucose solutions both total transmittance and diffuse reflectance of human sclera are changed insignificantly in contrast to collimated transmittance.

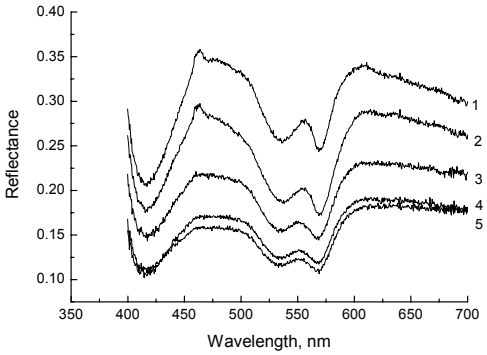

Fig. 5 The *in vivo* time-dependent reflectance spectra of the rabbit eye sclera measured concurrently with administration of 40%-glucose solution: 1 - 1 min, 2 - 4 min, 3 – 21 min, 4 - 25 min, 5 – 30 min after drop of the solution onto the eye surface [63].

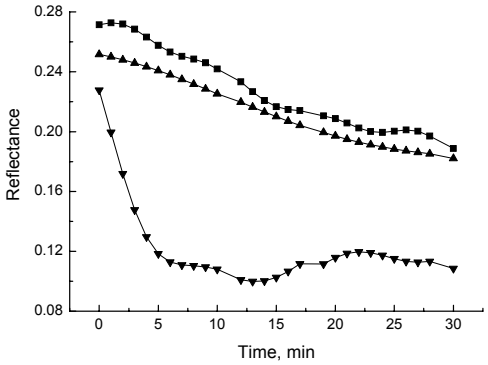

Fig. 6 The *in vivo* time-dependent reflectance of the rabbit eye sclera measured at 420 nm (down triangles), 630 nm (squares) and 700 nm (up triangles) concurrently with administration of 40%-glucose solution [63].

A significant decrease of the reflectance during the first five minutes of glucose administration is seen for rabbit sclera *in vivo* measurements. In this case, glucose solution with concentration 0.4 g/ml was used. Results of these measurements are presented in Figs. 5 and 6. Dips of reflectance at 420, 530 and 570 nm were caused by the blood hemoglobin absorption. Fast decay of reflectance at 420 nm (see Fig. 6) reflects blood dynamics in the scleral vessels providing a fast blood supply of the tissue bulk under glucose action. Such drop of reflectance is due to high absorption of the blood concentrated in the focus of inflammation caused by osmotic action of glucose and irradiating light of the spectrometer.

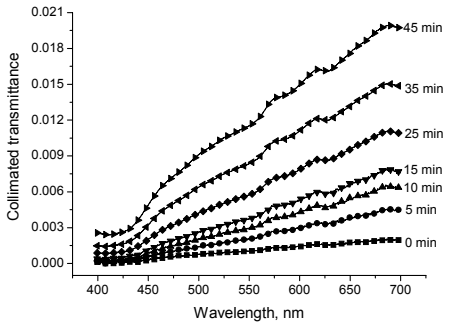

Fig. 7 The temporal collimated transmittance spectra of the rat skin measured concurrently with administration of glycerol [69].

Influence of glucose solution with concentration 0.4 g/ml and glycerol on the optical properties of skin are shown in Figs. 7-9. Figure 7 shows the collimated transmittance spectra of the rat skin sample measured for different time intervals concurrently with administration of glycerol. The collimated transmittance spectra of skin measured concurrently with administration of 40% glucose solution are similar to the spectra presented in Fig. 7. Figs. 8 and 9 present the time-dependent collimated

transmittance of the rat skin samples measured *in vitro* at different wavelengths concurrently with administration of glycerol (Fig. 8) [69] and 40%-glucose solution (Fig. 9) [73]. From these figures, we have seen that the osmotically active immersion liquids such as glycerol and the glucose solution can effectively control the optical properties of whole skin. At initial moment, the skin is very nontransparent for optical radiation tissue. Application of the osmotically active immersion liquids makes this tissue more transparent increase of skin collimated transmittance in about 100 folds for glycerol (Fig. 8) and in about 50 folds for 40% glucose solution at wavelength 700 nm during 45 min (Fig. 9).

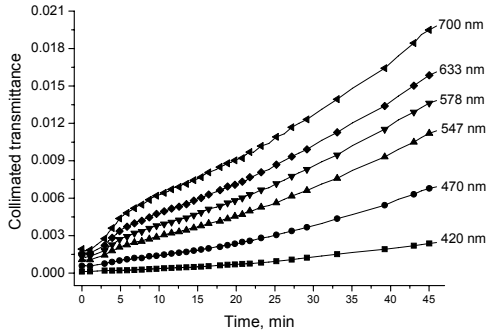

Fig. 8 The time-dependent collimated transmittance of the rat skin sample measured *in vitro* at different wavelengths concurrently with administration of glycerol [69].

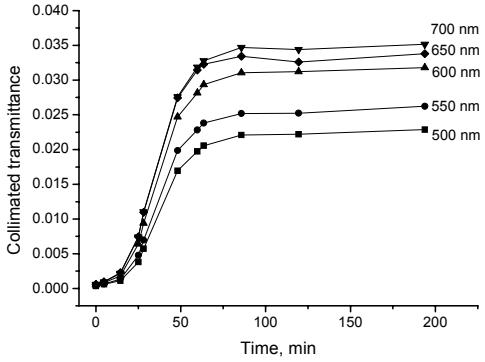

Fig. 9 The time-dependent collimated transmittance of the rat skin sample measured *in vitro* at different wavelengths concurrently with administration of 40%-glucose solution [73].

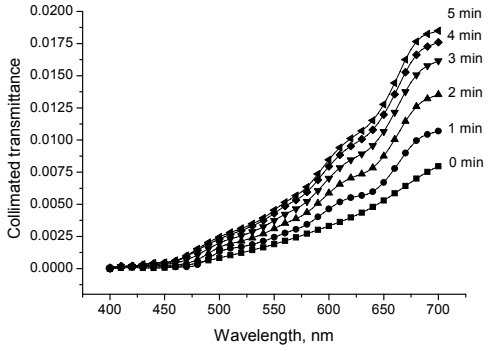

Fig. 10 The collimated transmittance spectra of the human dura mater sample measured concurrently with administration of mannitol solution at different time intervals.

To understand the mechanisms of the optical clearing of dura mater we have measured the collimated transmittance spectra concurrently with administration of the glucose and mannitol solutions. Glucose solutions with concentration of 0.2 and 0.4 g/ml were used in these experiments. Figure 10 illustrates the dynamics of the dura mater transmittance spectra measured at mannitol administration. It is easily seen that the untreated dura mater is poorly transparent for the visible light. Mannitol administration increases the collimated transmittance in the spectral range from 650 to 700 nm in average in about 2.5 folds at t = 5 min. The dura mater diffuse reflectance under action of the mannitol solution is decreased (see Fig. 11) in contrast to the total transmittance, which is changed insignificantly. From Fig. 11 one can easily see dips of reflectance at 420, 530 and 570 nm, which are caused by the blood absorption, since dura mater is well supplied by blood.

Figure 12 illustrates the dynamics of the collimated transmittance spectra of human dura mater measured concurrently with administration of glucose solution with concentration 0.2 g/ml. Symbols correspond to experimental data and solid lines correspond to data calculated by the developed model (see below, Section 5). Glucose administration increase the collimated transmittance in the spectral range from 650 to 700 nm in average in about 5 folds at t = 5 min. For glucose solution with concentration 0.4 g/ml, the collimated transmittance in the same spectral range, increases up to 16% during 5 minutes.

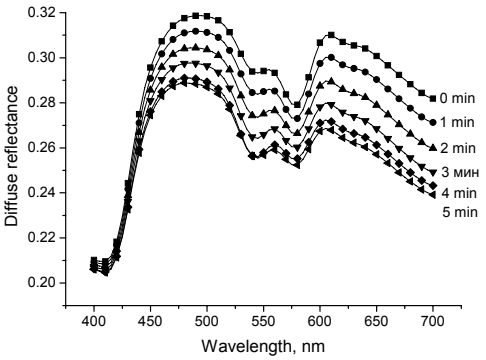

Fig. 11 The diffuse reflectance of the human dura mater sample measured concurrently with administration of mannitol solution at different time intervals.

From Fig. 12 one can see a good matching between experimental data (symbols) and approximating dependencies (solid lines) calculated in the framework of the model presented in Section 5. Insignificant differences between experimental and calculated data can be explained partially by inaccuracy of the measurements and simplicity of the used model, since the diffusion coefficient can change a little during penetration of the clearing agent into the tissue samples. Moreover, the dura mater samples are volume-inhomogeneous. The same reasons can be delivered to explain differences between the experimental and calculated data presented in Figs. 3 and 4.

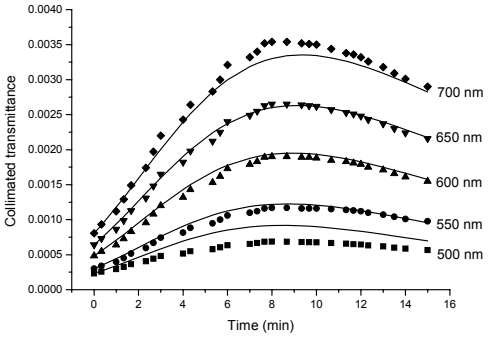

Fig. 12 The time-dependent collimated transmittance of the human dura mater sample measured at different wavelengths concurrently with administration of 20% glucose solution.

We have to underline that the clearing process has two stages (see Figs. 4, 12). At the beginning of the process we see the increase of the transmittance followed by saturation and even the decrease of the transmittance. Two competing processes take place. One of them is optical immersion - the matching of refractive indices of the tissue scatterers and the interstitial fluid that causes the decrease of the tissue scattering and, therefore, the increase of the collimated transmittance. Another one is the tissue swelling that causes the increase of the tissue thickness and thus the decrease of the transmittance. However, present experimental data show that the matching effect prevails, especially at the first stage of the optical clearing. It is well confirmed by the characteristic time of the swelling that is longer than the diffusion time. It is worth noting that usually swelling, caused by immersion agent impregnation, is not very important for *in vivo* tissue optical clearing, since living tissue has a high homeostasis degree, but for *in vitro* measurements this stage should be taken into account for the corrected determination of the diffusion coefficient. Typically, the saturation of the optical transmittance (reflectance) with time for *in vivo* measurements is caused by immersion liquid diffusion to the surrounding tissues, and it is difficult to provide a continuous supply of immersion liquid to the target tissue [63,69,73,72,77].

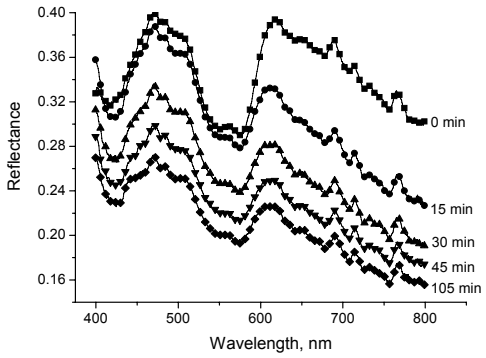

Fig. 13 *In vivo* reflectance spectra of rat skin measured at different time intervals after injection of 40%-glucose solution [73].

Since the developed algorithm for estimation of diffusion coefficients of osmotically active immersion liquids in tissues requires the knowledge of the tissue volume changes under action of these liquids (see Section 5) the temporal dependence of the tissue swelling index has been investigated using the time-dependent weight measurements. For quantitative assessment of the time-dependent weight measurements, the exponential association (Eq. 14 in Section 5) can be used.

Figure 13 shows dynamics of reflectance spectra at different time intervals of the rat skin after hypodermic injection of 40%-glucose solution [73]. Symbols correspond to experimental data. In the spectra the main absorption bands of blood are well seen. The decrease of the spectra corresponds to diffusion of the glucose solution from the injection place to the upper skin layers.

Figure 14 presents the dynamics of the change of skin reflectance at different wavelengths measured concurrently with administration of glycerol.

Analyzing the results of the experiments (glycerol was impregnated intradermally) one can see that dynamics of reflectance change has non-monotone character. We underline three stages of glycerol action on the skin and hypodermic tissues of the rat.

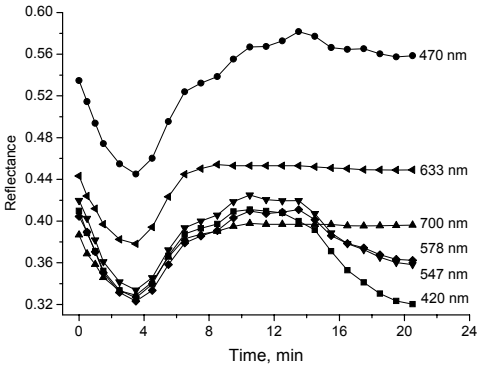

Fig. 14 The *in vivo* time-dependent reflectance of the rat skin measured at different wavelengths concurrently with administration of glycerol [69].

1. The first 3.5 minutes. Decreasing of the reflectance due to decreasing of the scattering of the tissue under action of glycerol is seen.
2. The second stage is from 3.5 to 13-13.5 min. The diffusion of glycerol into the ambient tissue, decreasing of glycerol concentration, increasing of tissue scattering and hence increasing of the reflectance takes place.
3. The third stage begins after about 13 minute of influence of glycerol on hypodermic tissues of the rat. The rush of blood to the place of interaction osmotically active substances with hypodermic tissues arises. Therefore, we observe decreasing of the reflectance in the absorption bands of blood (420, 547 and 578 nm).

Observable decreasing of the reflectance after 13 minutes of glycerol action (Fig. 14) is explained in the following way. In spite of the fact that glycerol often apply in a cosmetology, probably, it renders irritant action on hypodermic tissues of the rat, as apparently after 13 minutes of glycerol action.

It should be also noted that 1) we have watched a white ring around the injection puncture of about 1 cm in radius, when glucose solution or glycerol injected into skin dermis. The origin of this ring is due to

osmotically active liquids and tissue water interaction. The water diffuses from surrounding tissue and occupies some area around osmotic liquid injection, because of additional amount of water in this ring. The additional mismatch of refractive indices of the scatterers and interstitial fluid occurs, that is why this ring looks white. 2) It was shown that in the case of glycerol used as an active agent the irritation of hypodermic tissues after 13.5 min takes place [69]. It is expressed in the rush of blood to the place of injection. 3) In the case of using of the 40%-glucose solution as a clearing agent, the rush of blood is not observed. Hence, we can conclude that the 40%-glucose solution is more applicable than glycerol for *in vivo* optical clearing of the tissue in spite of the fact that glycerol has larger refractive index that the 40%-glucose solution.

Figures 15 and 16 show dynamics of reflectance spectra and time-dependent reflectance at different wavelengths of *in vivo* human skin injected by 40%-glucose solution [72]. It can be noted that the effect of tissue clearing was similar to that seen in the excised skin specimens [69,73]. From the spectra of reflectance of the skin it is well seen the main absorption bands of blood (Fig. 15).

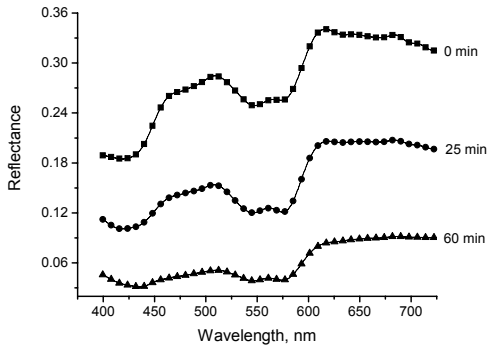

Fig. 15 The *in vivo* reflectance spectra of the human skin measured at administering of 40%-glucose solution in different time intervals after intradermic injection [72].

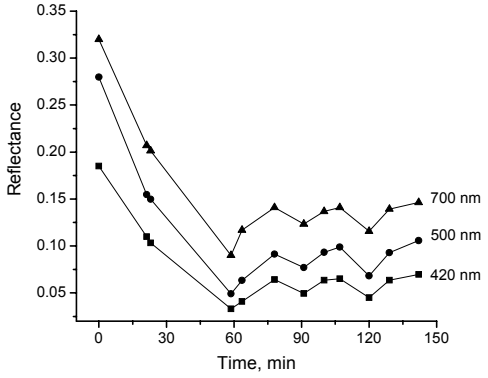

Fig. 16 The *in vivo* time-dependent reflectance of the human skin measured for different wavelengths at administering of 40%-glucose solution [72].

In Fig. 16, one can see that skin reflectance under glucose solution action is decreased. Glucose solution diffuse up to the skin surface and corresponding tissue clearing takes place. The glucose-injected region became more transparent. The area around the injection site that was unaffected by the glucose solution remained white and turbid. Reflectance of the skin decreases in about 3.8 times in an hour after clearing agent injection and then increases gradually, that shows the beginning of glucose diffusion from the observed area and corresponding reduction of tissue immersion. On the basis of the experiments, one can conclude that partial matching of refractive indices of the collagen fibers of dermis and the interstitial medium under action of 40%-glucose solution makes the main contribution to tissue clearing.

The obtained results have allowed for estimation the diffusion coefficient of 40%-glucose solution in the human skin as $D_g = (2.56 \pm 0.13) \cdot 10^{-6}$ cm^2/sec. The value of the diffusion coefficient was calculated by the method described in Ref. 72. It is in about 2-folds smaller then the diffusion coefficient of glucose in water at 37^{0}C, $D \approx 5.2 \cdot 10^{-6}$ cm^2/sec [151] and reflects the permeability of the collagen fiber network of the dermis.

It should be noted that skin has been transparent during a few hours. From the obtained value of the diffusion coefficient of glucose solution in the skin the time of impregnation of dermis layer with

thickness 0.9 mm by glucose solution, $\tau = l^2 / D_g \approx 53\,\text{min}$ can be estimated. It is the time of diffusion of glucose solution from the area of injection up to the epidermis, i.e. the time of skin clearing, what was observed experimentally. The second phase of tissue interaction with glucose is connected with taking down of the matching effect. It is determined by diffusion of glucose along the skin surface between a few orders less permeable two cellular layers – epidermal and subdermal fat cells. For the used aperture of the detector system, optical clearing was seen during a few hours, that is also corresponds to the measured diffusion coefficient of glucose in dermis.

5 Estimating diffusion coefficients of osmotically active immersion liquids in tissues

Method for estimation of diffusion coefficients of osmotically active liquids in tissues is based on the time-dependent measurement of collimated transmittance of tissue samples placed in immersion liquid. Schematic representation of diffusion of the osmotically active immersion liquid into the tissue sample and the geometry of light irradiation is presented in Fig. 17. The transport of an immersion liquid within the tissue can be described in the framework of the free diffusion model. We assume that the following approximations are valid for the transport process: 1) only concentration diffusion takes place, i.e. the exchange flux of osmotically active solution into the tissue and water from the tissue at a certain point within the tissue sample is proportional to the osmotically active substance concentration at this point; 2) the diffusion coefficient is constant over the entire sample volume.

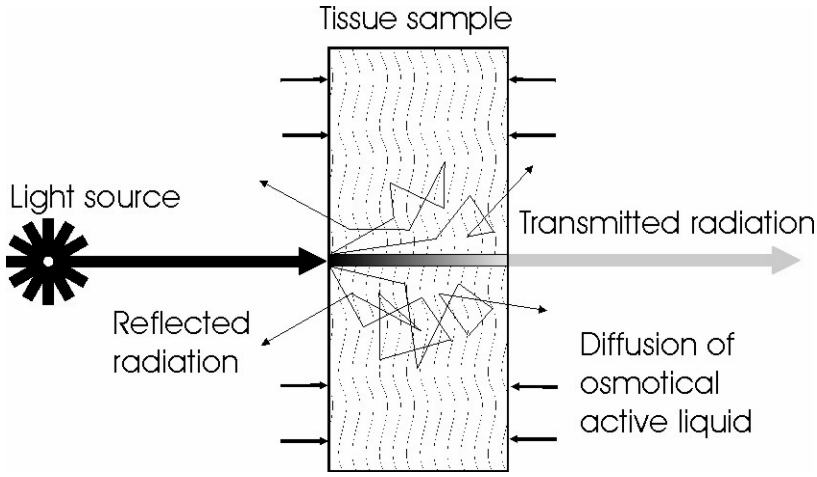

Fig. 17 Schematic representation of diffusion of osmotically active immersion liquid into the tissue sample and the geometry of light irradiation

Geometrically, the tissue sample is presented as a plane-parallel slab with a finite thickness. Since tissue samples in our experiments have rather big surface of 1×1 cm^2, which are much exceeding their thickness, the one-dimensional diffusion problem has been solved.

The one-dimensional diffusion equation of the immersion liquid transport has the form

$$\frac{\partial C(x,t)}{\partial t} = D \frac{\partial^2 C(x,t)}{\partial x^2}, \tag{3}$$

where $C(x,t)$ is the immersion liquid concentration; D is the diffusion coefficient, cm^2/sec ; t is time, sec; and x is the spatial coordinate, cm.

We also suppose that penetration of immersion liquid into a tissue sample does not change the immersion liquid concentration in the cuvette. This requirement has been met in our experiments since the immersion liquid volume in cuvette has been about 3000 mm^3 and the volume of the tissue samples has been less than 100 mm^3. The corresponding boundary conditions are as follows

$$C(0,t) = C(l,t) = C_0 = \text{const}, \tag{4}$$

where C_0 is the concentration of immersion liquid in the external volume (cuvette), l is the thickness of the sample, cm.

The initial conditions correspond to the absence of clearing agent (for example, glucose or mannitol) inside the tissue sample before its incubation in the immersion liquid

$$C(x,0) = 0 \tag{5}$$

for all inner points of the tissue sample.

Solution of Eq. 3 for a slab with a thickness l at the moment t with boundary (Eq. 4) and initial (Eq. 5) conditions has the form [100]

$$C(t) = C_0\left(1 - \frac{8}{\pi^2}\sum_{i=0}^{\infty}\frac{1}{(2i+1)^2}\exp\left(-(2i+1)^2 t\pi^2 D/l^2\right)\right), \tag{6}$$

where $C(t)$ is the volume-averaged concentration of osmotically active immersion liquid within tissue sample.

As a first approximation, we can rewrite Eq. 6 as

$$C(t) \approx C_0\left(1 - \exp\left(-t\pi^2 D/l^2\right)\right). \tag{7}$$

It is worth noting that Eq. 7 is very close to the equation describing diffusion through a partially permeable membrane and $C(t)$ corresponds to immersion liquid concentration in the interstitial fluid.

The time dependence of the refractive index of the interstitial fluid can be derived using the law of Gladstone and Dale, which states that the resulting value represents an average of the refractive indices of the components related to their volume fractions [88, 149]. Such dependence is defined as

$$n_I(t) = (1 - C(t))n_{base} + C(t)n_{osm}, \tag{8}$$

where n_{base} is the refractive index of the tissue interstitial fluid at the initial moment defined by Eq. 2, and n_{osm} is the refractive index of the glucose or mannitol solutions. Wavelength dependence of aqueous glucose solution can be estimated as $n_{osm}(\lambda) = n_w(\lambda) + 0.1515C$, where $n_w(\lambda)$ is the wavelength dependence of water, and C is the glucose concentration, g/ml [53]. The wavelength dependence of water has been presented by Kohl et al. [56] as

$$n_w(\lambda) = 1.3199 + \frac{6.878\times10^3}{\lambda^2} - \frac{1.132\times10^9}{\lambda^4} + \frac{1.11\times10^{14}}{\lambda^6}.$$

The optical model of tissue can be presented as a slab with a thickness l containing scatterers (collagen fibrils) – thin dielectric cylinders with an average diameter of 100 nm, which is considerably smaller than their lengths. The wavelength dependence of the refractive index of these cylinders is described by Eq. 1. These cylinders are located in planes that are parallel to the sample surfaces, but within each plane their orientations are random. These simplifications reduce considerably the difficulties in the description of light scattering by these tissues. For a thin dielectric cylinder in the Rayleigh-Gans

approximation of the Mie scattering theory the scattering cross-section $\sigma_s(t)$ for unpolarized incident light is given by

$$\sigma_s = \frac{\pi^2 a x^3}{8}\left(m^2-1\right)^2\left(1+\frac{2}{\left(m^2+1\right)^2}\right), \tag{9}$$

where *m* is the relative refractive index of the scattering particle, i.e. ratio of the refractive indices of the scatterers and the ground materials (i.e. interstitial fluid), and *x* is the dimensionless relative scatterers size, which is determined as $x = 2\pi a n_1 / \lambda$, where λ is the wavelength and *a* is the cylinder radius [87,89].

As a first approximation, we assume that during the interaction between the tissue and the immersion liquid the size of the scatterers does not change. This assumption is confirmed by the results presented by Huang and Meek [98]. In this case, all changes in the tissue scattering are connected with the changes of the refractive index of the interstitial fluid described by Eq. 8. The increase of the refractive index of the interstitial fluid decreases the relative refractive index of the scattering particles and, consequently, decreases the scattering coefficient. For non-interacting particles the scattering coefficient of a tissue is defined by the following equation

$$\mu_s(t) = N\sigma_s(t), \tag{10}$$

where $\mu_s(t)$ is the tissue scattering coefficient, *N* is number of the scattering particles (fibrils) per unit area and $\sigma_s(t)$ is the time-dependent cross-section of scattering (Eq. 9). The number of the scattering particles per unit area can be estimated as $N = \phi / \left(\pi a^2\right)$ [87], where ϕ is the volume fraction of the tissue scatterers. For typical fibrous tissues, such as sclera, dura mater and skin dermis, ϕ is usually equal to 0.3.

To take into account interparticle correlation effects which are important for tissues with densely packed scattering particles the scattering cross-section has to be corrected by the packing factor of the scattering particles, $(1-\phi)^3/(1+\phi)$ [96]. Thus, Eq. 10 has to be rewritten as

$$\mu_s(t) = \frac{\phi}{\pi a^2}\sigma_s(t)\frac{(1-\phi)^3}{1+\phi}. \tag{11}$$

Since glucose and mannitol solutions have pH different from pH of the interstitial fluid of the native tissue, placing tissues sample into the solutions produces the swelling process. The temporal dependence of the tissue sample volume can be described assuming that increasing tissue volume is the result of additional absorption of osmotically active liquid [98].

The temporal dependence of the swelling index $H(t)$ of the tissue sample can be calculated from weight measurements as

$$H(t) = \frac{M(t)-M(t=0)}{M(t=0)} = \frac{M_{osm}(t)}{M(t=0)} = \frac{V_{osm}(t)\times\rho_{osm}}{M(t=0)}, \tag{12}$$

where $M(t)$ is mass of the tissue sample in the different moments in the swelling process, $M_{osm}(t)$, $V_{osm}(t)$ and $\rho_{osm}(t)$ are mass, volume and density of osmotically active liquid absorbed by the tissue sample, respectively. Let $V(t)$ represent the volume of swelling tissue, then

$$V(t) = V(t=0) + V_{osm}(t) = V(t=0) + H(t)M(t=0)/\rho_{osm}\,. \tag{13}$$

Since the tissue swelling is connected with diffusion of osmotically active liquid into the tissue sample, the temporal dependence of swelling index can be approximated by the following phenomenological expression, which is very close to Eq. 7 describing the process of osmotically active liquid penetration into the tissue

$$H(t) = \frac{M(t) - M(t=0)}{M(t=0)} = A_w\left(1 - \exp\left(-t/\tau_{sw}\right)\right). \tag{14}$$

Therefore, the temporal dependence of tissue volume during osmotically active liquid action (Eq. 13) can be presented as

$$V(t) = V(t=0) + \frac{M(t=0)}{\rho_{osm}} A_w\left(1 - \exp\left(-t/\tau_{sw}\right)\right). \tag{15}$$

At the same time, Eq. 15 can be rewritten in a simpler form, i.e., as

$$V(t) = V(t=0) + A\left(1 - \exp\left(-t/\tau_{sw}\right)\right). \tag{16}$$

In this case A_w, A and τ_{sw} are some phenomenological constants describing swelling process caused by glucose or mannitol action. Volumetric changes of a tissue sample is mostly due to changes of its thickness $l(t)$, which can be expressed as

$$l(t) = l(t=0) + A^*\left(1 - \exp\left(-t/\tau_{sw}\right)\right). \tag{17}$$

where $A^* = A/S$, and S is the tissue sample area. Constants A and τ_{sw} can be obtained both from direct measurements of thickness or volume of tissue samples and from time-dependent weight measurements. In this study to estimate these constants, we used the time-dependent weight measurements of the tissue samples placed into osmotically active solutions. By least-squares method, the following parameters of the swelling index were obtained. For example, for the dura mater samples immersed in the mannitol solution, we have estimated parameter A_w as 0.21 and the parameter characterizing the swelling rate, i.e. τ_{sw} as 484 sec. For the dura mater samples immersed in glucose solution with concentration 0.2 g/ml, we have estimated parameter A_w as 0.20 and τ_{sw} as 528 sec.

By changing volume of a tissue the swelling produces the change of the volume fraction of the tissue scatterers, and thus the change of the scatterers packing factor and the numerical concentration, i.e. number of the scattering particles per unit area (see Eqs. 10 and 11). Taking into account Eq. 16, the temporal dependence of the volume fraction of the tissue scatterers is described as

$$\phi(t) = \frac{V_c}{V(t)} = \frac{\phi(t=0) \times V(t=0)}{V(t=0) + A\left(1 - \exp\left(-t/\tau_{sw}\right)\right)}, \tag{18}$$

where V_c is the volume of the tissue sample scatterers.

The collimated optical transmittance of the tissue sample impregnated by an immersion solution is defined as

$$T_c(t) = \left(1 - R_s\right)^2 \exp\left(-\left(\mu_a + \mu_s(t)\right) l(t)\right), \tag{19}$$

where R_s is the specular reflectance and μ_a is the absorption coefficient. The time-dependent scattering coefficient $\mu_s(t)$ and thickness $l(t)$ are defined by Eqs. 11 and 17, respectively. In the visible spectral

range, the absorption coefficient of a tissue is much less than the scattering coefficient except blood absorption bands. Since both glucose and mannitol do not have strong absorption bands within the wavelength range investigated, the changes of the tissue collimated transmittance can be described only by the behavior of the μ_s.

This set of equations describing the glucose or mannitol concentration dependent on time represents the direct problem. The reconstruction of the diffusion coefficient of the glucose or mannitol in tissue has been carried out on the basis of measurement of the temporal evolution of the collimated transmittance. The solution of the inverse problem was obtained by minimization of the target function:

$$F(D) = \sum_{i=1}^{N_t} \left(T_c\left(D, t_i\right) - T_c^*\left(t_i\right) \right)^2 ,$$

where $T_c\left(D,t\right)$ and $T_c^*\left(t\right)$ are the calculated and experimental values of the time-dependent collimated transmittance, respectively, and N_t is the number of time points obtained at registration of the temporal dynamics of the collimated transmittance. To minimize the target function the Levenberg-Marquardt nonlinear least-squares-fitting algorithm described in detail by Press et al. [150] was used. Iteration procedure repeats until experimental and calculated data were matched. As a termination condition of the iteration process, we have used the following expression:

$$\frac{1}{N_t} \sum_{i=1}^{N_t} \frac{\left| T_c\left(D, t_i\right) - T_c^*\left(t_i\right) \right|}{T_c^*\left(t_i\right)} \le 0.01 .$$

The mannitol and glucose diffusion coefficients in the human sclera and dura mater tissues were estimated using the temporal dependence of the collimated transmittance and method presented by us. Calculations were performed for ten wavelengths, and the obtained values of the diffusion coefficients have been averaged. The diffusion coefficients are presented in Table 1. It is well known that diffusion coefficient is increased with the increase of temperature of the solution. The temperature dependence was accounted for as $D\left(T_2\right) = D\left(T_1\right) \frac{T_2}{T_1} \frac{\eta\left(T_1\right)}{\eta\left(T_2\right)}$ [151]. Where $D\left(T\right)$ is diffusion coefficient at temperature T and $\eta\left(T\right)$ is viscosity of the solution. Corrected to temperature 37^0C values of the diffusion coefficients also are presented in Table1.

It was expected that diffusion coefficients measured for tissues are less than for solutions. For example, Peck et al. [103] have found for mannitol diffusion in phosphate-buffered saline at temperature 37^0C $D_M = \left(9.03 \pm 0.3\right) \times 10^{-6}$ cm^2/sec. Under the same conditions, for sucrose $D_S = 7.45 \times 10^{-6}$ cm^2/sec [104] and for raffinase $D_R = \left(5.72 \pm 0.1\right) \times 10^{-6}$ cm^2/sec [103]. The diffusion coefficients of glucose and mannitol in water are 5.2×10^{-6} cm^2/sec (at 15^0C) and 6.05×10^{-6} cm^2/sec (at 20^0C), respectively [151]. At 37^0C the diffusion coefficient of glucose in water is 9.59×10^{-6} cm^2/sec, the diffusion coefficient of mannitol in water is 9.61×10^{-6} cm^2/sec and these values are well matched with the data presented by Peck et al. [103].

Differences between the diffusion coefficients of these substances in water and in tissue are connected with the structure and composition of the tissue interstitial fluid, since the scleral and dura mater interstitial fluid contains the proteins, proteoglycans and glycoproteins. The differences between the diffusion coefficients obtained in this paper and presented by other authors are explained by the differences in structure and properties of the investigated tissues. The differences can be due to the various experimental and calculation methods and thus are rather in an acceptable range.

Table 1. The experimentally measured and temperature corrected diffusion coefficients

Tissue	*Osmotically active immersion liquid*	*Diffusion coefficient,* $\mathrm{cm}^2/\mathrm{sec}$	*Corrected diffusion coefficient,* $\mathrm{cm}^2/\mathrm{sec}$
Sclera	Glucose solution (20%)	$(0.57 \pm 0.09) \times 10^{-6}$	$(0.91 \pm 0.09) \times 10^{-6}$
Sclera	Glucose solution (30%)	$(1.47 \pm 0.36) \times 10^{-6}$	$(2.34 \pm 0.36) \times 10^{-6}$
Sclera	Glucose solution (40%)	$(1.52 \pm 0.05) \times 10^{-6}$	$(2.42 \pm 0.05) \times 10^{-6}$
Dura mater	Glucose solution (20%)	$(1.63 \pm 0.29) \times 10^{-6}$	$(2.59 \pm 0.29) \times 10^{-6}$
Dura mater	Mannitol solution	$(1.31 \pm 0.41) \times 10^{-6}$	$(2.08 \pm 0.41) \times 10^{-6}$
Skin (in vivo)	Glucose solution (40%)	$(2.56 \pm 0.13) \times 10^{-6}$	

Conclusion

The presented experimental results have shown that control of the optical properties of tissues is a useful method to increase the ability of light penetration into a tissue and, consequently, to improve the optical imaging depth. Changes of the collimated transmittance indicate that administration of the osmotically active immersion liquids into a fibrous tissue allows one to control its optical characteristics effectively. Basing on temporal dependence of the collimated transmittance of the human sclera and dura mater samples and the present model, glucose and mannitol diffusion coefficients in tissue interstitial fluid at 20^0C were estimated.

Acknowledgements

The research described in this publication has been made possible in part by Award "Leading Scientific Schools" number 00-15-96667 of the Russian Basic Research Foundation and by Award No. REC-006 of the U.S. Civilian Research & Development Foundation for the Independent States of the Former Soviet Union (CRDF), and Ministry of Education of Russian Federation. The authors thank Dr. S.V. Eremina for the help in manuscript translation to English.

References

1 Hebden J C, Arridge S R, Delpy D T, *Phys Med Biol*, 42 (1997) 825.

2 Arridge S R, Hebden J C, *Phys Med Biol*, 42 (1997) 841.

3 Tuchin V V, *Tissue optics: light scattering methods and instruments for medical diagnosis* (SPIE Press, TT38, Bellingham, Washington), 2000.

4 Demos S G, Radousky H R, Alfano R R, *Opt Express*, 7 (2000) 23.

5 Ntziachristos V, Hielscher A H, Yodh A G, Chance B, *IEEE Transact medic imaging*, 20 (2001) 470.

6 Tuchin V V (ed), *Handbook of Optical Biomedical Diagnostics* (SPIE Press, PM107, Bellingham, Washington), 2002.

7 Jacques S L, Ramella-Roman J C, Lee K, *J Biomed Opt*, 7 (2002) 329.

8 Mehrubeoglu M, Kehtarnavaz N, Marquez G, Duvic M, Wang L V, *Appl Opt*, 41 (2002) 182.

9 Fridolin I, Lindberg L-G, *Phys Med Biol*, 45, (2000) 3765.

10 Fridolin I, Hansson K, Lindberg L-G, *Phys Med Biol*, 45 (2000) 3779.

11 Backman V, Gurjar R, Badizadegan K, Itzkan I, Dasari R R, Perelman L T, Feld M S, *IEEE J Quant Electron*, 5 (1999) 1019.

12 Bigio I J, Bown S G, Briggs G, Kelley C, Lakhani S, Pickard D, Ripley P M, Rose I G, Saunders C, *J Biomed Opt*, 5 (2000) 221.

13 Heusmann H, Kolzer J, Mitic G, *J Biomed Opt*, 1 (1996) 425.

14 Troy T L, Page D L, Sevick-Muraca E M, *J Biomed Opt*, 1 (1996) 342.

15 Utzinger U, Brewer M, Silva E, Gershenson D, Blast R C, Follen M, Richards-Kortum R, *Lasers Surg Med*, 28 (2001) 56.

16 Zellweger M, Grosjean P, Goujon D, Monnier Ph, van den Berg H, Wagnieres G, *J Biomed Opt*, 6 (2001) 41.

17 Zuluaga A F, Drezek R, Collier T, Lotan R, Follen M, Richards-Kortum R, *J Biomed Opt,* 7 (2002) 398.

18 Abels C, Fickweiler S, Weiderer P, Baumler W, Hofstadter F, Landthaler M, Szeimies R-M, *Arch Dermatol Res*, 292 (2000) 404.

19 Altshuler G B, Anderson R R, Manstein D, Zenzie H H, Smirnov M Z, *Lasers Surg Med*, 29 (2001) 416.

20 Cunliffe W J, Goulden V, *British J Dermatol*, 142 (2000) 855.

21 Douplik A, Stratonnikov A A, Loshchenov V B, Lebedeva V S, Derkacheva V M, Vitkin A, Rumyanceva V D, Kusmin S G, Mironov A F, Luk'Yanets E A, *J Biomed Opt*, 5 (2000) 338.

22 Fehr M K, Hornung R, Degen A, Schwarz V A, Fink D, Haller U, Wyss P, *Lasers Surg Med*, 30 (2002) 273.

23 Hongcharu W, Taylor C R, Chang Y, Aghassi D, Suthamjariya K, Anderson R R, *J Invest Dermatol*, 115 (2000) 183

24 Krishnamurthy S, Powers S, Witmer P, Brown T, *Lasers Surg Med*, 27 (2000) 224.

25 Papageorgiou P, Katsambas A, Chu A, *British J Dermatol*, 142 (2000) 973.

26 Nemati B, Rylander III H G, Welch A J, *Appl Opt*, 35 (1996) 3321.

27 Nemati B, Dunn A, Welch A J, Rylander III H G, *Appl Opt*, 37 (1998) 764.

28 Chance B, Mayevsky A, Guan B, Zhang Y, *In: Oxygen Transport to Tissue XIX*, Harrison D K and Delpy D T, editors, (Plenum Press, New York), 1997, p 457.

29 Hueber D M, Franceschini M A, Ma H Y, Zhang Q, Ballesteros J R, Fantini S, Wallace D, Ntziachristos V, Chance B, *Phys Med Biol,* 46 (2001) 41.

30 Liu H, Boas D A, Zhang Y, Yodh A G, Chance B, *Phys Med Biol*, 40 (1995) 1983.

31 Meglinski I V, Matcher S J, *Physiol Measurem*, 23 (2002) 741.

32 Nitzan M, Babchenko A, Khanokh B, Taitelbaum H, *J Biomed Opt*, 5 (2000) 155.

33 Ramanujam N, Vishnoi G, Hielscher A, Rode M, Forouzan I, Chance B, *J Biomed Opt*, 5 (2000) 173.

34 Smith M H, Denninghoff K R, Hillman L W, Chipman R A, *J Biomed Opt*, 3 (1998) 296.

35 Stratonnikov A A, Loschenov V B, *J Biomed Opt*, 6 (2001) 457.

36 Tuchin V V, *J Biomed Opt,* 4 (1999) 106.

37 Vishnoi G, Hielscher A H, Ramanujam N, Chance B, *J Biomed Opt*, 5 (2000) 163.

38 Zourabian A, Siegel A, Chance B, Ramanujan N, Rode M, Boas D A, *J Biomed Opt*, 5 (2000) 391.

39 Sliney D, Wolbarsht M, *Safety with lasers and others optical sources. A comprehensive handbook* (Plenum Press, New York), 1980.

40 Liu H, Beauvoit B, Kimura M, Chance B, *J Biomed Opt,* 1 (1996) 200.

41 Vorob'ev N S, Podgaetskii V M, Smirnov A V, Tereshchenko S A, Tomilova L G, *Quant Electron*, 29 (1999) 261.

42 Tuchin V V, Maksimova I L, Zimnyakov D A, Kon I L, Mavlutov A H, Mishin A A, *J Biomed Opt,* 2 (1997) 401.

43 Vargas G, Chan E K, Barton J K, Rylander III H G, Welch A J, *Lasers Surg Med,* 24 (1999) 133.

44 Vargas G, Chan K F, Thomsen S L, Welch A J, *Lasers Surg Med,* 29 (2001) 213.

45 Wang R K, Elder J B, *Lasers Surg Med,* 30 (2002) 201.

46 Bornhop D J, Contag C H, Licha K, Murphy C J, *J Biomed Opt*, 6 (2001) 106.

47 Zimnyakov D A, Tuchin V V, *Quant Electron*, 32 (2002) 849.

48 Boas D A, O'Leary M A, Chance B, Yodh A G, *Appl Opt*, 36 (1997) 75.

49 Chen Y, Mu C, Intes X, Chance B, *Opt Express*, 9 (2001) 212.

50 Dunn A K, Smithpeter C, Welch A J, Richards-Kortum R, *Appl Opt*, 35 (1996) 3441.

51 Rol P O, *Optics for transscleral laser applications*, *Ph D Thesis*, (Swiss Federal Institute of Technology, Zurich, Switzerland), 1991.

52 Cilesiz I F, Welch A J, *Appl Opt*, 32 (1993) 477.

53 Maier J S, Walker S A, Fantini S, Franceschini M A, Gratton E, *Opt Lett,* 19 (1994) 2062.

54 Beauvoit B, Kitai T, Chance T, *Biophys J*, 67 (1994) 2501.

55 Chance B, Liu H, Kitai T, Zhang Y, *Anal Biochem,* 227 (1995) 351.

56 Kohl M, Esseupreis M, Cope M, *Phys Med Biol,* 40 (1995) 1267.

57 Chan E, Menovsky T, Welch A J, *Appl Opt*, 35 (1996) 4526.

58 Chan E K, Sorg B, Protsenko D, O'Neil M, Motamedi M, Welch A J, *IEEE J Quant Electron*, 2 (1996) 943.

59 Bruulsema J T, Hayward J E, Farrell T J, Patterson M S, Heinemann L, Berger M, Koschinsky T., Sandahl-Christiansen J, Orskov H, Essenpreis M, Schmelzeisen-Redeker G, Bocker D, *Opt Lett*, 22 (1997) 190.

60 Qu J, Wilson B C, *J Biomed Opt*, 2 (1997) 319.

61 Demos S G, Wang W B, Alfano R R, *Appl Opt,* 37 (1998) 792.

62 Bashkatov A N, Genina E A, Kochubey V I, Tuchin V V, Sinichkin Yu P, *Proc SPIE*, 3726, (1999) 403.

63 Bashkatov A N, Tuchin V V, Genina E A, Sinichkin Yu P, Lakodina N A, Kochubey V I, *Proc SPIE*, 3591 (1999) 311.

64 Tuchin V V, Bashkatov A N, Genina E A, Kochubey V I, Lakodina N A, Simonenko G V, Sinichkin Yu P, Proshina Yu M, Razumikhina N A, *Proc SPIE*, 3863 (1999) 10.

65 Maksimova I L, Zimnyakov D A, Tuchin V V, *Opt Spectros*, 89 (2000) 78.

66 Zimnyakov D A, Maksimova I L, Tuchin V V, *Opt Spectros,* 88 (2000) 936.

67 Bashkatov A N, Genina E A, Kochubey V I, Lakodina N A, Tuchin V V, *Proc SPIE*, 3908 (2000) 266.

68 Bashkatov A N, Genina E A, Kochubey V I, Sinichkin Yu P, Korobov A A, Lakodina N A, Tuchin V V, *Proc SPIE*, 4162 (2000) 182.

69 Bashkatov A N, Genina E A, Korovina I V, Kochubey V I, Sinichkin Yu P, Tuchin V V, *Proc SPIE*, 4224 (2000) 300.

70 Genina E A, Bashkatov A N, Lakodina N A, Murikhina S A, Sinichkin Yu P, Tuchin V V, *Proc SPIE*, 4001 (2000) 255.

71 Genina E A, Bashkatov A N, Lakodina N A, Kosobutsky I D, Bogomolova N V, Altshuler G B, Tuchin V V, *Proc SPIE*, 4224 (2000) 312.

72 Tuchin V V, Bashkatov A N, Genina E A, Sinichkin Yu P, Lakodina N A, *Tech Physics Lett,* 27 (2001) 489.

73 Bashkatov A N, Genina E A, Korovina I V, Sinichkin Yu P, Novikova O V, Tuchin V V, *Proc SPIE*, (2001) 4241 223.

74 Tuchin V V, Bashkatov A N, Maksimova I L, Sinichkin Yu P, Simonenko G V, Genina E A, Lakodina N A, *Proc SPIE*, 4427 (2001) 41.

75 Genina E A, Bashkatov A N, Sinichkin Yu P, Lakodina N A, Korovina I V, Simonenko G V, Tuchin V V, *Proc SPIE*, 4432 (2001) 97.

76 Esenaliev R O, Larin K V, Larina I V, Motamedi M, *Opt Lett*, 26 (2001) 992.

77 Bashkatov A N, Genina E A, Sinichkin Yu P, Tuchin V V, *Proc SPIE*, (2002) 4623 144.

78 Bashkatov A N, *Control of tissue optical properties by means of osmotically active immersion liquids, Ph D Thesis*, (Saratov State University, Saratov), 2002.

79 Genina E A, Bashkatov A N, Sinichkin Yu P, Kochubey V I, Lakodina N A, Altshuler G B, Tuchin V V, *J Biomed Opt,* 7 (2002) 471.

80 Tuchin V V, Bashkatov A N, Genina E A, Sinichkin Yu P, *Proc SPIE*, 4611 (2002) 54.

81 Tuchin V V, Xu X, Wang R K, *Appl Opt*, 41, (2002) 258.

82 Tuchin V V, *Proc SPIE*, 4536 (2002) 273.

83 Yao L, Cheng H, Luo Q, Zhang W, Zeng S, Tuchin V V, *Proc SPIE,* 4536 (2002) 147.

84 Galanzha E I, Tuchin V V, Luo Q M, Chen H Y, *Proc SPIE*, 4707 (2002) 244.

85 Meglinskii I V, Bashkatov A N, Genina E A, Churmakov D Yu, Tuchin V V, *Quant Electron*, 32 (2002) 875.

86 Meglinski I V, Bashkatov A N, Genina E A, Churmakov D Y, Tuchin V V, *Laser Physics*, 13 (2003) 65.

87 Cox J L, Farrell R A, Hart R W, Langham M E, *J Physiol,* 210 (1970) 601.

88 Freund D E, McCally R L, Farrell R A, *J Opt Soc Am A,* 3 (1986) 1970.

89 Bohren C F, Huffman D R, *Absorption and Scattering of Light by Small Particles* (Wiley, New York), 1983.

90 Graaff R, Aarnoudse J G, Zijp J R, Sloot P M A, de Mul F F M, Greve J, Koelink M H, *Appl Opt*, 31 (1992) 1370.

91 Bevilacqua F, Marquet P, Coquoz O, Depeursinge C, *Appl Opt*, 36 (1997), 44.

92 Dunn A K, *Light scattering properties of cells, Ph D Thesis*, (Univ. Texas at Austin), 1997.

93 Mourant J R, Fuselier T, Boyer J, Johnson T M, Bigio I J, *Appl Opt*, 36 (1997) 949.

94 Borovoi A G, Naats E I, Oppel U G, *J Biomed Opt*, 3 (1998) 364.

95 Mourant J R, Freyer J P, Hielscher A H, Eick A A, Shen D, Johnson T M, *Appl Opt*, 37 (1998) 3586.

96 Schmitt J M, Kumar G, *Appl Opt,* 37 (1998) 2788.

97 Wang R K, *J Mod Opt,* 47 (2000) 103.

98 Huang Y, Meek K M, *Biophys J,* 77 (1999) 1655.

99 Beck R E, Schultz J S, *Biochem Biophys Acta*, 255 (1972) 272.

100 Kotyk A, Janacek K, *Membrane transport: an interdisciplinary approach* (Plenum Press, New York), 1977.

101 Blank I H, Moloney J, Emslie A G, Simon I, Apt C, *J Invest Dermatol*, 82 (1984), 188.

102 Sennhenn B, Giese K, Plamann K, Harendt N, Kolmel K, *Skin Pharmacol*, 6, (1993), 152.

103 Peck K D, Ghanem A H, Higuchi W I, *Pharm Res,* 11 (1994) 1306.

104 Inamori T, Ghanem A H, Higuchi W I, Srinivasan V, *Intern J Pharmaceutics,* 105 (1994) 113.

105 Bertram R, Pernarowski M, *Biophys J*, 74 (1998) 1722.

106 Gribbon P, Hardingham T E, *Biophys J,* 75 (1998) 1032.

107 Yaroslavskaya A N, Yaroslavsky I V, Otto C, Puppels G J, Guindam H, Vrensen G F J M, Greve J, Tuchin V V, *Biophysics*, 43 (1998) 109.

108 Alanis E E, Romero G G, Martinez C C, *Opt Eng*, 39 (2000) 744.

109 Papadopoulos S, Jurgens K D, Gros G, *Biophys J,* 79 (2000) 2084.

110 Kamholz A E, Schilling E A, Yager P, *Biophys J*, 80 (2001) 1967.

111 Olmsted S S, Padgett J L, Yudin A I, Whaley K J, Moench T R, Cone R A, *Biophys J,* 81 (2001) 1930.

112 Kusba J, Li L, Gryczynski I, Piszczek G, Johnson M, Lakowicz J R, *Biophys J*, 82 (2002) 1358.

113 Komai Y, Ushiki T, *Invest Ophthalmol & Visual Sci*, 32 (1991) 2244.

114 Maurice D, *In: The Eye,* Devison H, ed, (Marcel Dekker, New York), 1969, p. 489.

115 Spitznas M, *Am J Ophthalmol*, 71 (1971) 68.

116 Legeza S G, Privalov A I, *Ophthalmic J (Russia)*, 3 (1985) 170.

117 Trier K, Olsen S B, Ammitzboll T, *Acta Ophtalmol*, 69 (1990) 304.

118 Culav E M, Clark C H, Merrilees M J, *Phys Therapy,* 79 (1999) 308.

119 Zatulina N I, *Ophtalmol J (Russia)*, 5 (1988) 300.

120 Avetissow E S, Andeeva L D, Chooshilova-Maslova I P, *Ophtalmol Bull (Russia)*, 1 (1979) 24.

121 Thale A, Tillman B, *Anat Anz*, 175 (1993) 215.

122 Vaezy S, Clark J I, *J Microscopy*, 175 (Pt.2) (1994) 93.

123 Schaefer H, Redelmeier T E, *Skin barrier* (Karger, Basel, Switzerland), 1996, p.310.

124 Marks R, Barton S P, *In: Stratum corneum*, Marks R, Plewig G, editors, (Springer, Berlin), 1983, p.175.

125 Wester R C, Maibach H I, *In: Percutaneous Absorption*, Bronaugh R L and Maibach H I, editors, (Decker, Basel, Switzerland), 1989, p. 111.

126 Grove G L, Lavker R M, Holze E, Kligman A M, *J Soc Cosmet Chem*, 32 (1981) 15.

127 Harvell J D, Maibach H I, *J Am Acad Dermatol*, 31 (1994) 1015.

128 Saint Leger D, Francois A M, Leveque J L, Stoudemayer T J, Grove G L, Kligman A M, *Dermatologica*, 32 (1988) 1025.

129 Montagna W, Kligman A M, Carlisle K S, *Atlas of Normal Human Skin* (Springer Verlag, New York), 1992.

130 Odland G F, *In: Physiology, Biochemistry and Molecular Biology of the Skin,* Goldsmith L A, ed, (Oxford University Press, Oxford), 1991, I, p. 3.

131 Ryan T J, *In: Physiology, Biochemistry and Molecular Biology of the Skin*, Goldsmith L A, ed, (Oxford University Press, Oxford), 1991, II, 1019.

132 Eckert R L, *Physiol Rev*, 69 (1989) 1316.

133 Steinert P M, *J Invest Derm*, 100 (1993) 729.

134 Elias P M, Menon G K, *Adv Lipid Res*, 24 (1991) 1.

135 Downing D T, Stewart M E, Wertz P W, Strauss J S, *In: Dermatology in General Medicine,* Fitzpatrick T B, Eisen A Z, Wolff K, Freedberg I M, Austen K F, editors, (McGraw-Hill, New York), 1993, p. 210.

136 Warner R R, Myers M C, Taylor D A, *J Invest Derm*, 90 (1988) 218.

137 von Zglinicki T, Lindberg M, Roomans G M, Forsling B, *Acta Derm Venerol*, 73 (1993) 340.

138 Anderson R R, *In: Clinical Photomedicine*, Lim H W, Soter N A, editors, (Dekker, New York), 1993, p. 19.

139 Chedekel M R, *In: Melanin: Its Role in Human Photoprotection*, Zeise L, Chedekel M R and Fitzpatrick T B, editors, (Overland Park: Valdenmar), 1995, p.11.

140 Uitto J, *In: Dermatology in General Medicine,* Fitzpatrick T B, Eisen A Z, Wolff K, Freedberg I M, Austen K F, editors, (McGraw-Hill, New York), 1993, p. 221.

141 Ryan T J, *In: Biochemistry and Physiology of the Skin*, Goldsmith L A, ed, (Oxford University Press, Oxford), 1983, II, p. 817.

142 Braverman I M, *J Invest Derm*, 93 (1089) 2.

143 Stuttgen G, Forssmann W G, *In: Normal and Pathologic Physiology of the Skin. Part III,* Stuttgen G, Spier H W, Schwarz E, editors, (Springer, Berlin), 1981, p. 379.

144 Ryan T J, *J Invest Dermatol*, 93 (1989), 18.

145 Zyablov V I, Shapovalov Yu N, Toskin K D, Tkach V V, Zherebovski V V, Georgievskaya L S, *Archive of anatomy, histology and embryology (Russia),* 3 (1982) 29.

146 Baron M A, Mayorova N A, *Atlas of functional stereomorphology of brain membranes* (Medicine, Moscow), 1982.

147 Spacek J, *Atlas of ultrastructural neurocytology* (http://synapses.bu.edu/atlas/), 2000.

148 Vertel B M, *Color Textbook of Histology* (http://www.finchcms.edu/anatomy/), 2001.

149 Leonard D W, Meek K M, *Biophys J,* 72 (1997) 1382.

150 Press W H, Tuekolsky S A, Vettering W T, Flannery B P, *Numerical recipes in C: the art of scientific computing* (Cambridge University Press, Cambridge), 1992.

151 Grigoriev I S, Meylikhov E Z (editors), *Physical values: Handbook* (EnergoAtomIzdat, Moscow), 1991.